

Diffusion as Reasoning: Enhancing Object Goal Navigation with LLM-Biased Diffusion Model

Yiming Ji, Yang Liu, Zhengpu Wang, Boyu Ma, Zongwu Xie, and Hong Liu

Abstract—The Object Goal Navigation (ObjectNav) task requires the agent to navigate to a specified target in an unseen environment. Since the environment layout is unknown, the agent needs to perform semantic reasoning to infer the potential location of the target, based on its accumulated memory of the environment during the navigation process. Diffusion models have been shown to be able to learn the distribution relationships between features in RGB images, and thus generate new realistic images. In this work, we propose a new approach to solving the ObjectNav task, by training a diffusion model to learn the statistical distribution patterns of objects in semantic maps, and using the map of the explored regions during navigation as the condition to generate the map of the unknown regions, thereby realizing the semantic reasoning of the target object, i.e., diffusion as reasoning (DAR). Meanwhile, we propose the *global target bias* and *local LLM bias* methods, where the former can constrain the diffusion model to generate the target object more effectively, and the latter utilizes the common sense knowledge extracted from the LLM to improve the generalization of the reasoning process. Based on the generated map in the unknown region, the agent sets the predicted location of the target as the goal and moves towards it. Experiments on Gibson and MP3D show the effectiveness of our method.

Index Terms—diffusion model; object goal navigation; semantic reasoning; common sense knowledge

I. INTRODUCTION

Embodied navigation, which requires an agent to use visual sensing to actively interact with its environment and perform navigation tasks, has seen rapid development driven by large-scale photorealistic domestic scene datasets [1], [2], [3] and advanced high-performance simulators [4], [5]. As a specific form of embodied navigation, Object Goal Navigation (ObjectNav) [6] is regarded as a key technology for enabling robotic intelligence. In ObjectNav task, the agent is placed in an unknown environment and is required to navigate to a user-specified object category (e.g. sofa) based on visual observations. Since the environment is unseen, when the target object is not visible, the agent needs to infer the potential locations of the target.

The intelligence of an embodied navigation agent is primarily manifested in its semantic understanding and reasoning capabilities of the world (e.g., TVs are in the living room, ovens are in the kitchen, and chairs are near tables). Prior work has made some research progress in how to learn and incorporate the contextual relationships between objects into ObjectNav systems. Some methods extract relationship information among objects, regions, or rooms, and leverage this

prior knowledge to enhance the visual representation of end-to-end navigation models [7], [8]. Other end-to-end approaches directly learn how to map the visual representation to actions by interacting with the environment [9], [10]. However, end-to-end methods implicitly embed semantic prior knowledge and simultaneously learn localization, mapping, and path planning in an implicit manner, which leads to the problems of high computational load and limited generalization in unseen environments.

Alternatively, modular methods tend to use a long-term goal policy module instead of the frontier exploration module, while also retaining the mapping and path planning modules in the traditional pipeline [11], [12], [13], [14]. However, the key issue remains how to represent and learn the contextual relations in the long-term goal policy module to perform semantic reasoning about the target location.

Some modular approaches use supervised learning to directly learn target relations, such as predicting the nearest potential frontier on a local map [12], estimating the distance to the target [15], or anticipating the target’s coordinates [16]. Other methods use the distance to the target as a reward to train modular-based reinforcement learning (RL) approaches [14]. However, both approaches fail to fully exploit the geometric and semantic cues in the map, as they implicitly and independently learn object relations. Therefore, learning the cooperative relationships among multiple objects in the scene has proven to be more reliable [13]. Furthermore, the ability of Large Language Models (LLMs) to extract and integrate knowledge for robotics has been widely studied [17]. The inherent common-sense knowledge in LLMs significantly improves the success rate of ObjectNav systems. However, zero-shot, training-free approaches [18] that rely solely on LLMs offer limited reliability when only sparse semantic information is available, as the reasoning capability of LLMs using their common-sense knowledge is diminished [19].

To alleviate the above problems, we propose an approach named DAR (Diffusion As Reasoning). This method combines the strengths of data-driven modular techniques with common-sense knowledge from LLMs about semantic and spatial relationships, enhancing the efficiency of ObjectNav systems.

The proposed DAR method uses Denoising Diffusion Probabilistic Models [20] (DDPM), conditioning on the agent’s memory of the environment to generate reliable semantic content in unknown areas. Following the self-supervised learning setup of DDPM, we replace the original 3-channel RGB data with semantic maps of the class channels, scaling up the denoising model accordingly. Our DAR is trained to predict pixel values in unexplored regions by leveraging both explo-

All authors are with State Key Laboratory of Robotics and Systems, Harbin Institute of Technology. (Corresponding author: Yang Liu).
jiyiming@alu.hit.edu.cn, liuyanghit@hit.edu.cn

ration memory and common sense knowledge. Exploration memory represents a local semantic map built from the agent’s visual observations of the environment. Unlike standard image datasets, ObjectNav has limited training scene quantity and diversity. To improve generalization, we also incorporate general knowledge from LLMs (e.g. GPT-4 [21]). Unlike existing method [22], the DAR approach does not require frequent LLM queries during navigation for valuable decisions. Instead, it relies on a knowledge graph, pre-extracted from LLMs, that represents object relationships.

In summary, our study has the following main contributions:

- We use a DDPM to generate semantic maps, trained on public datasets [3], [23]. We propose a *global target bias* method to generate more specific types of objects, which controls the channel bias of the initial noise in the sampling process.
- We pre-extract a knowledge graph from LLMs based on semantic and spatial relevance, and introduce a *local LLM bias* method to inject common-sense knowledge into the sampling process. This guides the DDPM to generate more specific objects in particular regions, according to the suggestions provided by the LLM.
- We propose the **DAR** method as a modular-based solution to the ObjectNav problem. By using the trained denoising model, we integrate globally and locally biased initial noise and use an existing local semantic map as a condition to predict the object distribution in unexplored regions within a certain range. This enables semantic reasoning with a diffusion model, predicting potential locations of the target object.

II. RELATED WORK

A. Object goal navigation

ObjectNav aims to navigate an agent to a specific object in a previously unknown indoor scene. Existing approaches fall into three categories [24]: end-to-end, modular, and zero-shot methods. End-to-end methods use reinforcement learning (RL) [25] or imitation learning (IL) [26] to map observations directly to actions. Previous RL-based methods focus on learning object relations [27], visual representations [28], auxiliary tasks [29], and data augmentation [30] to improve navigation. However, these approaches face challenges in real-world application as they require simultaneous localization, mapping, and planning, with additional difficulties in transferring from simulation to real-world environments due to perceptual differences [31].

Unlike end-to-end methods, modular approaches [12], [13] break down ObjectNav tasks into separate components: mapping [11], long-term goal reasoning [19], and path planning [32]. The mapping module provides a general representation that separates perception from reasoning and planning, making it more suitable for real-world applications.

Zero-shot methods involve navigating to unseen targets that only appear during testing [33]. Existing approaches [34], [35] use Vision Language Models (VLMs) and Large Language Models (LLMs) to provide prior knowledge about these unseen targets. However, relying solely on pre-trained VLMs or LLMs

limits reliability, especially when the robot detects limited semantic information. Our DAR is a modular method that uses a diffusion model to design a novel long-term goal reasoning module. It also incorporates the common-sense knowledge from LLMs, avoiding the reliability issues that come with relying solely on LLMs.

B. Visual semantic reasoning

In ObjectNav, visual semantic reasoning is meant to provide high-level information about the location of the target object. Considering the two extremes, when the semantic reasoning module is highly inefficient, the navigation system tends to explore aimlessly until it has traversed the entire room. On the other hand, when the semantic reasoning module can accurately and reliably compute the target’s position, it can greatly improve the efficiency of the navigation system by avoiding exploration in ineffective regions and directly reaching the target.

SK Ramakrishnan [12] proposed two complementary potential functions as a semantic reasoning approach to determine long-term goals in frontier areas. L2M [36] actively imagines environmental layouts beyond the agent’s field of view and uses uncertainty in the semantic classes of unobserved areas to choose long-term goals. S Zhang [13] proposed training with an MAE mechanism to leverage both episodic observations and general knowledge for generating semantic maps of unknown areas, enabling long-term goal reasoning. This approach is similar to our DAR method. However, the MAE mechanism involves random masking of the established local map, causing information loss. In contrast, our DAR method fully utilizes the local map to guide a diffusion model for generating high-quality semantic maps.

C. Diffusion models

Diffusion models are a type of deep generative model that have recently gained attention for tasks like image generation [37], image translation [38], inpainting [39], and editing [40]. They consist of a forward diffusion stage, where Gaussian noise is gradually added to the data, and a reverse diffusion stage, where the model learns to recover the original data step by step.

Denoising Diffusion Probabilistic Models (DDPMs), a key type of diffusion model, demonstrated the ability to generate high-quality images, with benefits like full distribution coverage, a stable training objective, and easy scalability [20][41][42]. Our DAR model leverages DDPMs to learn the distribution of objects in rooms, enabling the generation of high-quality room maps. We also adapt DDPM’s image inpainting capabilities to predict unknown areas based on known conditions, offering a novel approach to the semantic reasoning needed in ObjectNav systems.

III. METHODOLOGY

A. Task Definition

The ObjectNav task involves an agent navigating to an instance of a given object category (e.g., toilet) in an unknown environment. At the start of each episode, the agent

is randomly placed. At each timestep t , it receives egocentric RGB-D observations, target object information, and its current pose (x, y, θ) . The agent can perform one of four discrete actions: *move forward*, *turn left*, *turn right*, or *stop*. The agent autonomously executes a stop action when it determines the task is complete. An episode is considered successful if, within a given number of steps, the agent stops at a position where the distance to the target is below a threshold (e.g., 1m) and the target is visible in its egocentric view.

Our method builds on the modular ObjectNav architecture, which typically constructs an accumulating semantic map during navigation. The semantic map ($m_t \in \mathbb{R}^{(N_o+N_s) \times H \times W}$) uses multiple channels to represent different classes: N_o for occupancy classes (occupied and free), and N_s for object classes, with H and W as the map dimensions. This map accumulates observed object layouts of the environment from timesteps 0 to t .

However, since the semantic map is built from partial observations, it represents only a subset (i.e., a local map) of the entire environment. When the target is not visible, the agent must estimate the unobserved surroundings based on learned contextual relationships among objects to infer the target’s likely location.

B. Self-supervised Diffusion Learning

In the field of RGB image generation, trained diffusion models can learn the latent statistical distribution of image features. We have observed that the spatial distribution of objects in indoor scenes also follows certain statistical patterns. Since diffusion models can generate high-quality RGB images, they should, with sufficient training, also be able to generate high-quality maps of room object distributions. Building on this idea, we used a room semantic map dataset to train an unconditional diffusion model.

In the diffusion process, the noisy data x_t at step t is calculated as follows:

$$x_t = \sqrt{\hat{\beta}_t} \cdot x_0 + \sqrt{\left(1 - \hat{\beta}_t\right)} \cdot z_t, z_t \sim \mathcal{N}(0, \mathbf{I}) \quad (1)$$

Where $\hat{\beta}_t = \prod_{i=1}^t \alpha_i$, $\alpha_t = 1 - \beta_t$ and $t \in \{1, 2, \dots, T\}$, with the original map x_0 and a fixed variance schedule β_t , the noise x_t can be sampled by Eq. 1.

If the variance schedule $(\beta_t)_{t=1}^T$ makes $\hat{\beta}_T \rightarrow 0$, then x_T approaches the standard Gaussian distribution, namely $x_T \rightarrow \mathcal{N}(0, \mathbf{I})$. The training process is represented by reversing the forward diffusion process. By training a neural network model to predict the noise corresponding to each time step, the noise can then be removed one by one, gradually recovering the original data x_0 . This process is described as Eq. 2, where θ represents the parameters of the neural network model, and the network takes noisy data x_t and time step t as input to predict the mean $\mu_\theta(x_t, t)$ and covariance $\Sigma_\theta(x_t, t)$.

$$p_\theta(x_{t-1}|x_t) = \mathcal{N}(x_{t-1}; \mu_\theta(x_t, t), \Sigma_\theta(x_t, t)) \quad (2)$$

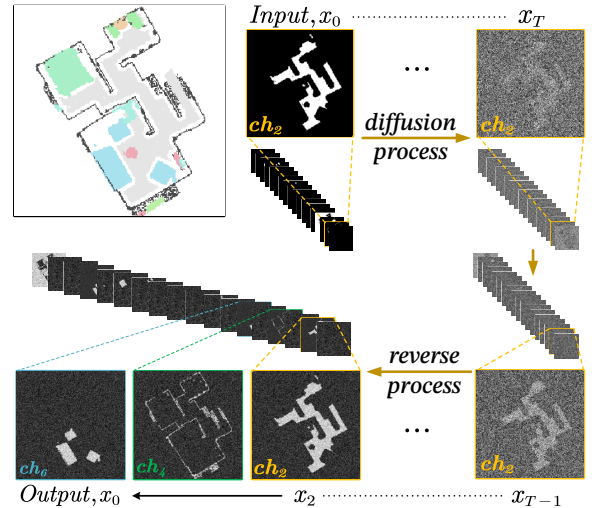


Figure 1: Diffusion learning process.

Ho et al. [20] proposed a simplified method, where the covariance $\Sigma_\theta(x_t, t)$ is fixed to a constant value and the mean $\mu_\theta(x_t, t)$ is rewritten as a function of noise, as follows:

$$\mu_\theta = \frac{1}{\sqrt{\alpha_t}} \cdot \left(x_t - \frac{1 - \alpha_t}{\sqrt{1 - \hat{\beta}_t}} \cdot z_\theta(x_t, t) \right) \quad (3)$$

With the simplified training objective, as follows:

$$\mathcal{L}_{vib} = \mathbb{E}_{t \sim [1, T]} \mathbb{E}_{x_0 \sim p(x_0)} \mathbb{E}_{z_t \sim \mathcal{N}(0, \mathbf{I})} \|z_t - z_\theta(x_t, t)\|^2 \quad (4)$$

Where \mathbb{E} is the expected value. As a result, the neural network model no longer needs to predict both the mean and covariance simultaneously, but only needs to estimate the noise $z_\theta(x_t, t)$ corresponding to x_t .

As shown in Figure 1, the input x_0 contains 18 binary semantic category channels (using the GIBSON dataset as an example). Additionally, we rescale the room semantic maps from the dataset to a resolution of 256×256 . Following the training process of diffusion models for RGB images, the model architecture is consistent with guided-diffusion [37], with increased depth and channel count of the U-Net model. The trained diffusion model can generate a regularized RGB image from noise. Similarly, by using 18-channel Gaussian noise as input, the model progressively removes the noise and ultimately generates a semantic map. Note that the output of the denoising model does not produce a standard multi-channel binary-valued semantic map. Therefore, we use the argmax operation to post-process the results and obtain the output shown in Figure 3.

Next, we raise another question: How can we make the generated semantic maps from the diffusion model contain more ‘specified’ objects? This problem is similar to the field of conditional image generation, but it is not feasible to train a conditional denoising model using classification ideas on multi-channel semantic maps, as the meaning of the map lies in the distribution of the objects it contains, and considering the overall category of the map is meaningless. In this paper, we propose a simple and effective way to address this question.

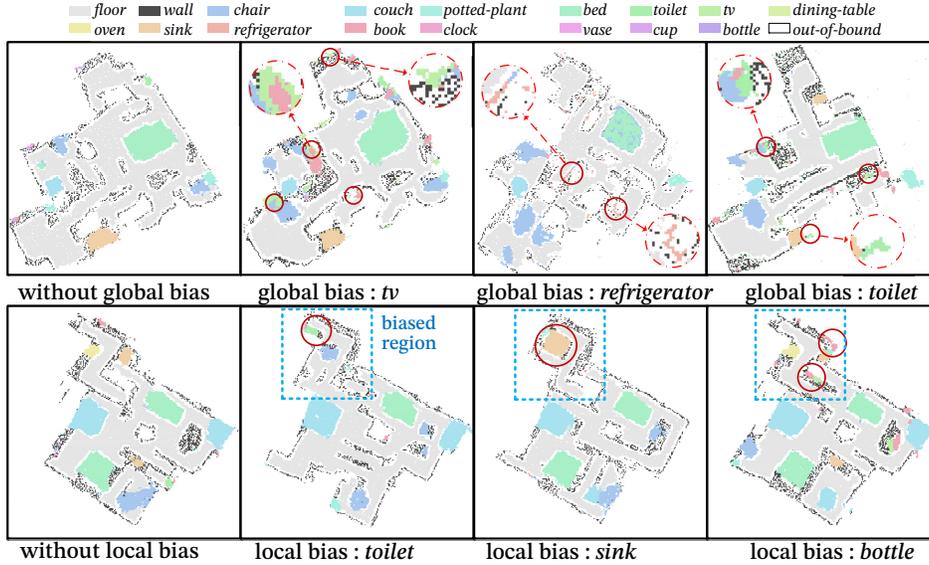


Figure 2: The effect of global and local biases.

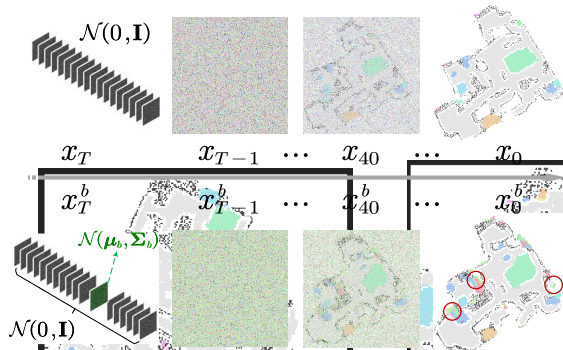


Figure 3: The effect of global target bias.

For the target channel, the noise is replaced with a biased Gaussian noise distribution with mean μ_b and covariance Σ_b , while the other channels remain unchanged. We refer to this process as 'global target bias'. Compared to using standard Gaussian noise across all channels, using the target-biased noise as the initial input results in the denoising model generating outputs containing more objects corresponding to the target channel.

As shown in Figure 3, applying bias to the *TV* channel during the sampling process results in more intermediate noise representing *TV*, visible as green pixels in sections x_{T-1}^b and x_{40}^b . This eventually leads to the generation of a map containing more *TV* instances, which are marked with red circles in Figure 3. In contrast, the map generated without bias during sampling does not contain any *TV* at all.

The two sampling processes shown in Figure 3 used the same torch random seed to demonstrate the effectiveness of the global target bias. Additionally, even with the bias towards *TV* channel, the model did not randomly generate a chaotic *TV* grid, but rather generated the *TV* near *book*, *chair*, and *couch*,

which aligns with the actual patterns. This suggests that after the global target bias, the model was able to generate more of the target objects according to the learned distribution of room objects. More examples of global target bias generation can be seen in Figure 2. All the maps were generated by the diffusion model.

C. Semantic Reasoning with Local Map Condition

The observed local semantic map can be used as a condition to guide the diffusion model in generating the object distribution in the unknown regions, thereby enabling semantic reasoning of the target objects. The local map established for the explored regions is denoted as x . After cropping and scaling preprocessing, the unknown area in x constitute the mask m . The known grid is represented as $x \odot (1 - m)$, and the corresponding unknown region is denoted as $x \odot m$. We apply the RePaint [39] method, using Eq. 5 for the known region and Eq. 6 for the unknown region.

$$x_{t-1}^{known} \sim \mathcal{N} \left(\sqrt{\hat{\beta}_t} \cdot x_0, (1 - \hat{\beta}_t) \cdot \mathbf{I} \right) \quad (5)$$

$$x_{t-1}^{unknown} \sim \mathcal{N} (\mu_\theta(x_t, t), \Sigma_\theta(x_t, t)) \quad (6)$$

As shown in Figure 5, x_{t-1} and x_{t-1}^g represent the sampled result from the local map and the model trained in the previous section, respectively.

$$x_{t-1} = (1 - m) \odot x_{t-1}^{known} + m \odot x_{t-1}^{unknown} \quad (7)$$

They are combined through the process represented by Eq. 7 and participate in the reverse process, ultimately generating a reasonable semantic content distribution in the unknown region of the local map.

D. Enhancing Generation with LLM Bias

Although we found that the diffusion model can effectively generate the object distribution in unknown regions, the object goal navigation domain lacks large-scale datasets, making it difficult to achieve satisfactory generalization through supervised training. Recently, the ability of knowledge extraction and integration within Large Language Models (LLMs) for robotics has been extensively investigated. LLMs can provide agents with common sense knowledge about the environment, which can improve the success rate of object goal navigation tasks [22][19].

The research in Section III-B showed that by changing the channel bias of the initial noise in the denoising model for map generation, the richness of each object in the final semantic map can be controlled. This bias is global. In contrast, this section proposes a local bias method that uses LLMs to predict the object distribution in different regions and applies specific biases in those regions, thereby exerting control over the diffusion model’s map generation process. We collect the

	chair	sofa	pillow	table	bed	TV	dining table	sofa	refrigerator	book	cup	apple
chair	0.00	0.00	0.00	0.00	0.00	0.00	0.00	0.00	0.00	0.00	0.00	0.00
sofa	0.00	0.00	0.00	0.00	0.00	0.00	0.00	0.00	0.00	0.00	0.00	0.00
pillow	0.00	0.00	0.00	0.00	0.00	0.00	0.00	0.00	0.00	0.00	0.00	0.00
table	0.00	0.00	0.00	0.00	0.00	0.00	0.00	0.00	0.00	0.00	0.00	0.00
bed	0.00	0.00	0.00	0.00	0.00	0.00	0.00	0.00	0.00	0.00	0.00	0.00
TV	0.00	0.00	0.00	0.00	0.00	0.00	0.00	0.00	0.00	0.00	0.00	0.00
dining table	0.00	0.00	0.00	0.00	0.00	0.00	0.00	0.00	0.00	0.00	0.00	0.00
sofa	0.00	0.00	0.00	0.00	0.00	0.00	0.00	0.00	0.00	0.00	0.00	0.00
refrigerator	0.00	0.00	0.00	0.00	0.00	0.00	0.00	0.00	0.00	0.00	0.00	0.00
book	0.00	0.00	0.00	0.00	0.00	0.00	0.00	0.00	0.00	0.00	0.00	0.00
cup	0.00	0.00	0.00	0.00	0.00	0.00	0.00	0.00	0.00	0.00	0.00	0.00
apple	0.00	0.00	0.00	0.00	0.00	0.00	0.00	0.00	0.00	0.00	0.00	0.00

Figure 4: Prompts and object association matrix.

common sense knowledge by querying the LLM with positive-negative prompts [22] and Chain-of-Thought (CoT) prompting technology [43]. Additionally, we query the LLM from the dimensions of semantic and spatial relevance, and then fuse the statistical results of these two dimensions to generate the common sense knowledge matrix M_{CS} . Subsequently, we set the diagonal values of M_{CS} to 0. Our goal is to use M_{CS} to calculate the object distribution tendency for a specific frontier point in the local map. The frontier points are defined as the edges between explored free-spaces and unexplored areas on the local semantic map [12]. Specifically, based on the coordinates of the frontier point f_p , we calculate the normalized distance score between all objects in the local map $f_s = [s_0, s_1, \dots, s_n]^T$. The score s_i represents the distance score of object i relative to f_p , and the closer the distance, the closer the score is to 1. Taking the Gibson dataset [3] as an example, $n = 14$, and the score for objects not present in the map is 0.

Next, we compute $M_{CS} \times f_s$ by matching the object proximity sequence corresponding to the frontier point in the local map with each row in M_{CS} . The object with the highest overall score ($\max(M_{CS} \times f_s)$) is taken as the prediction result. If the diagonal values of M_{CS} are 1, the prediction results will tend to generate the objects closest to the frontier point f_p , which, for instances, would lead to generating more

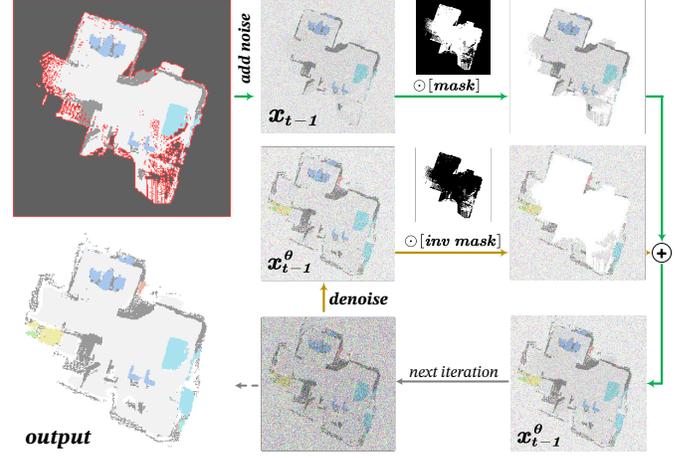


Figure 5: Generating maps of unknown regions using the local map as a condition.

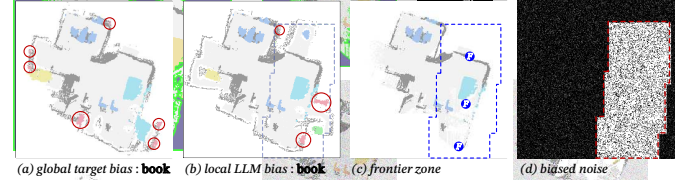


Figure 6: The proposed local LLM bias method.

chair near around *chair*. Therefore, we set the diagonal values to zero to reduce the weight of the nearest objects, allowing the model to predict a greater variety of objects in the frontier regions.

For example, in Figure 6, the three frontier points (denoted as F) are predicted by M_{CS} to most likely contain *book*. The 100×100 region filled around F constitutes the frontier zone. When generating the initial noise for the diffusion model, we apply a bias in the *book* channel within the frontier zone, while the regions outside the frontier zone and the other object channels still use the unbiased $\mathcal{N}(0, \mathbf{I})$ noise.

Figure 6-a shows the results of applying global bias, where noise is applied globally in the *book* channel. In contrast, Figure 6-b only applies noise bias within the frontier zone, which constrains the model to generate more of the target objects in the biased region.

E. Object Goal Navigation with DAR

At each timestamp t during navigation, the agent constructs a local semantic map m_t based on sensor input. The semantic map contains multiple channels, with each channel composed of binary-valued pixels. The values in the unobserved regions are 0 across all channels.

The trained diffusion model only allows for the prediction of map data at a resolution of 256×256 . Therefore, we crop the minimum bounding box of the known region from the input m_t , as shown by the blue dashed box in Figure 7. We then rescale the box region to a size of $256/\epsilon$ and pad it with zeros to 256×256 , generating the processed map m_t^p . The value

of ϵ represents the range of unknown regions that the DAR model is used to predict. We set $\epsilon = 120\%$. Next, we generate the initial noise with biases for the sampling process based on m_t^p . First, we apply the global target bias introduced in Section III-A. Then computing the frontier points F_i of m_t^p , and utilize the common sense knowledge matrix M_{CS} extracted from the LLM, as described in Section III-C, to estimate the most likely objects for each F_i . Finally, we apply the local bias.

The biased noise goes through the denoising process described in Section III-B, gradually producing a semantic map m_t^d within the unknown area of the m_t^p . In the m_t^d , non-zero values in the target channel indicate the predicted potential location of the target object by the DAR model. These coordinates are restored to the local map m_t through inverse resizing and used as the long-term goal g_t .

It is worth noting that in the initial stage of navigation or when the sensors receive limited information, even with the introduction of global target bias, the map generated by the DAR model in the unknown regions may not contain the target object. In other words, the DAR model may not provide valuable information to the navigation system. In such cases, we set the long-term goal to the nearest frontier point.

Once the long-term goal is set, the agent just needs to move from its current location to the goal g_t . Following previous work [11], we use the Fast Marching Method [32] to calculate the shortest path between the current location and the goal. The local policy then follows this path by taking deterministic actions to guide the agent.

While the diffusion model can effectively predict the object distribution in unknown regions, its nature also makes the DAR method computationally expensive. To address this drawback, we do not call the DAR method to reason about the long-term goal at every timestamp. Instead, we adopt a strategy where we only perform the reasoning when the current location is near the g_t , or when the agent is moving away from g_t . Subsequent experiments have shown the effectiveness of this approach, as the DAR model can still provide a significant performance boost to the object goal navigation system, even with fewer reasoning steps.

IV. EXPERIMENT

A. Experimental setup

Dataset. We evaluate our DAR on standard ObjectNav datasets: Gibson [3], Matterport3D (MP3D) [1], and Habitat-Matterport3D (HM3D) [23]. For Gibson and MP3D, we follow the setup of [12] and [13]. Specifically, for Gibson, we use 25 training and 5 validation scenes from the Gibson tiny split. For MP3D, we use 56 training and 11 validation scenes, with 21 goal categories and 2,195 validation episodes. For HM3D, we follow [44], using 80 training and 20 validation scenes, with 6 goal categories and 2,000 validation episodes.

Evaluation metrics. For evaluating the navigation performance, we adopt three standard metrics following [11] and [12]: 1) SR: the ratio of success episodes. 2) SPL: the success rate weighted by the path length, which measures the efficiency of the path length. 3) DTS: the distance to the goal at the end of the episode.

Table I: Comparisons of different map generation method

ID	Model	LLM	RS	Map generation		Navigation	
				IoU (%) \uparrow	Recall (%) \uparrow	SR (%) \uparrow	SPL (%) \uparrow
1	UNet	-	-	19.28	47.36	67.5	37.8
	SGM (ViT-B)	-	-	25.45	79.23	74.1	39.8
	SGM (ViT-B)	GPT-4	-	39.47	87.33	77.4	43.8
2	DAR (1K steps)	-	\times	24.28	75.31	74.3	39.7
	DAR (2K steps)	-	\times	26.61	82.53	76.7	40.4
	DAR (0.5K steps)	-	\checkmark	30.63	74.59	77.6	42.8
3	DAR (0.5K steps)	-	\times	22.11	73.12	73.2	38.7
	DAR (0.2K steps)	-	\checkmark	22.31	72.96	69.5	39.3
	DAR (0.2K steps)	-	\times	17.84	65.44	65.6	36.1
4	DAR (0.5K steps)	GPT-4	\checkmark	40.12	86.58	78.2	44.2

Implementation details. For the self-supervised diffusion learning of DAR, we take room semantic maps from the Gibson and MP3D datasets, randomly rotate, scale, and crop them to 256x256 size for training samples. We use a DDPM model based on UNet, with 2 BigGAN residual blocks.

B. Comparisons with previous map completion methods.

Previous works [36] train a UNet [45] to predict unobserved regions directly from a single semantic top-down map. Similar to our approach, SGM [13] leverages MAE [46] to train and integrate LLMs’ general knowledge for generating unobserved regions.

As shown in Table I, we compare the proposed DAR method (a mask-agnostic approach) with the Unet method and SGM (which utilizes ViT and learns with randomly masked sub-maps). In the experiments, as illustrated in Figure 8, we use a 75% random mask consistent with SGM, using the known areas as conditions to generate the masked region maps. To examine the contribution of M_{CS} to object prediction, we set up 16×16 patches and randomly mask 25% of the map. For each masked patch, we use the method in Section III-D to call M_{CS} to predict the possible objects, and then calculate the recall of the semantic map based solely on M_{CS} predictions. The M_{CS} extracted from the LLM does not contain any prior information about the rooms in the Gibson or other datasets, so it requires a sufficient amount of known areas to make effective judgments. Therefore, we only mask 25% of the regions in the experiments in Table II.

As shown in Table II, using the COT and positive-negative prompting technology to extract the M_{CS} matrix representing the associative relationships between objects from the LLM can effectively improve the performance of the DAR model in navigation.

C. Diffusion process analysis.

The proposed DAR model uses DDPM to reason about the object distribution in unknown regions by pre-training the DDPM on the semantic map dataset. We set up various diffusion steps and obtain the training loss decay curves shown in Figure 9. It can be seen that the higher the diffusion steps, the faster the model’s training loss decays and the lower the final convergence level, indicating that increasing the diffusion steps helps the model learn and generate more reasonable room semantic maps. This can also be observed from the second and third groups (id=2 and 3) in Table I. However, more diffusion steps during sampling means more computational time.

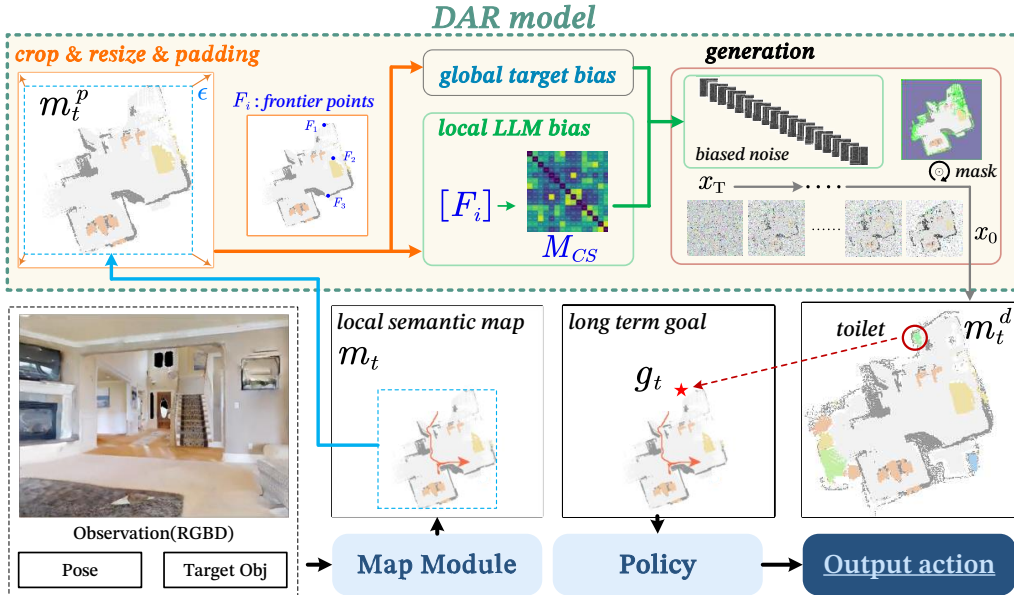


Figure 7: Workflow of the proposed DAR method during navigation.

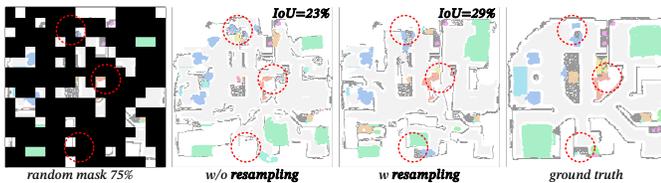


Figure 8: The DAR model reconstructing the map of the masked region.

The REPAINT method introduces a resampling strategy to harmonize the model’s input, producing higher-quality images. We apply this approach to enhance the realism of the generated maps. The ‘RS’ in Table I represents whether the resampling process is used. We find that a 0.5k steps pre-trained model with resampling can achieve higher map generation and navigation performance compared to a 1k steps model without resampling.

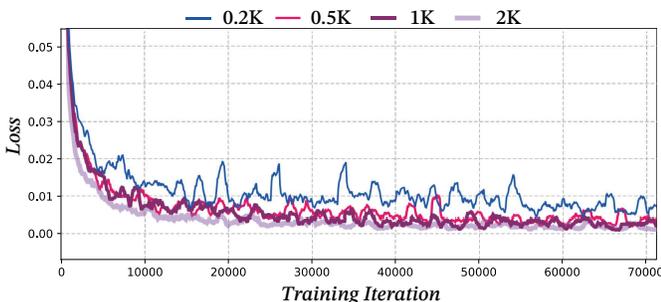


Figure 9: Training loss curves for different diffusion steps.

D. Visualization of navigating with DAR.

We follow the SGM configuration, and at the beginning of the navigation stage, the agent’s collected environmental information is insufficient to support accurate visual reasoning, so we use the original exploration strategy. As more scenes are observed, the DAR model successfully predicts the position of the target (toilet), even though it has not yet been observed. During the navigation process, DAR continuously predicts the object distribution in the unknown area based on the agent’s accumulated environmental memory, and provides a long-term goal to guide the exploration direction. It is worth noting that due to the inherent characteristics of the diffusion model, DAR’s semantic reasoning contains a certain degree of randomness. Even in the same scene, with the same starting position and target, each call to DAR for navigation will yield different results.

As shown in Figure 10, although the paths obtained are not completely identical, overall, DAR still significantly improves the efficiency of ObjectNav. From Figure 11, it can also be seen that the DAR model not only successfully predicts the potential location of the target object during the navigation process, but also estimates the approximate locations of other objects and their context. There is still some deviation between the predicted target position and the true position by DAR, but we believe this is acceptable, as even humans cannot precisely locate unseen objects in an unseen scene.

These two visualizations show that our DAR effectively expands limited local maps by generating unobserved regions, enabling the agent to infer the target’s location.

E. Ablation study.

We verify the global target bias and local LLM bias methods in the DAR model, and obtain the results shown in Table III. Introducing an exploration strategy early in navigation

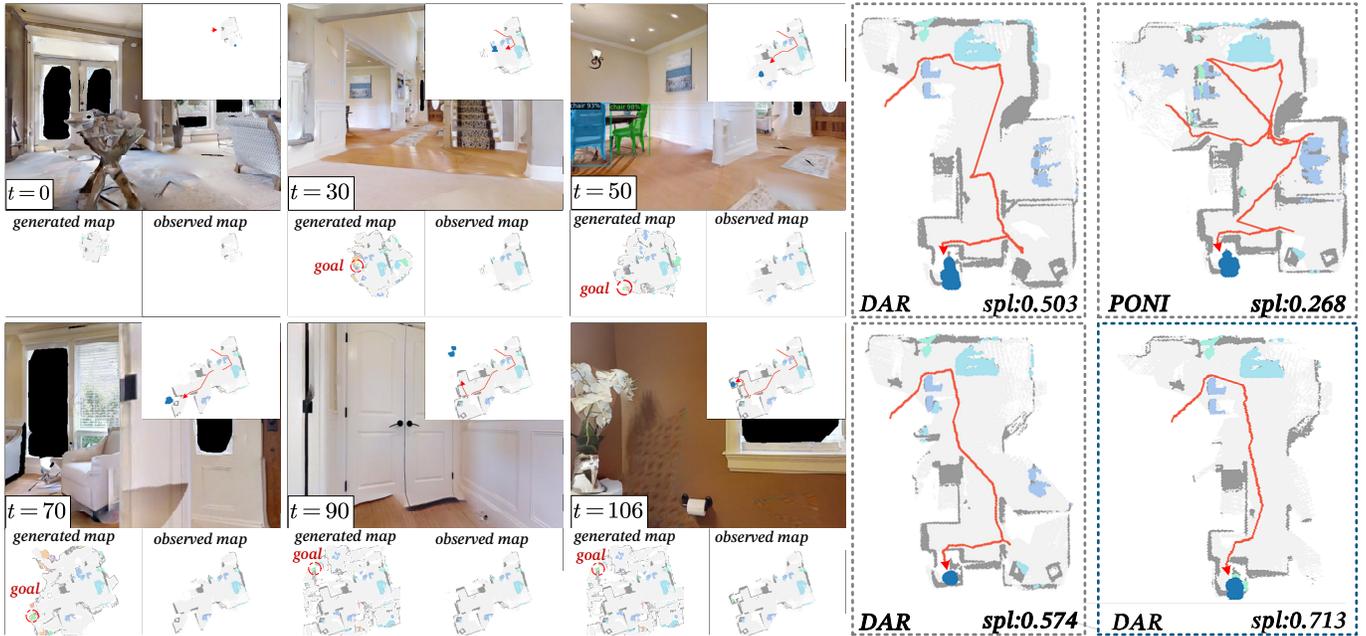


Figure 10: Visualization of navigation using the proposed DAR method.

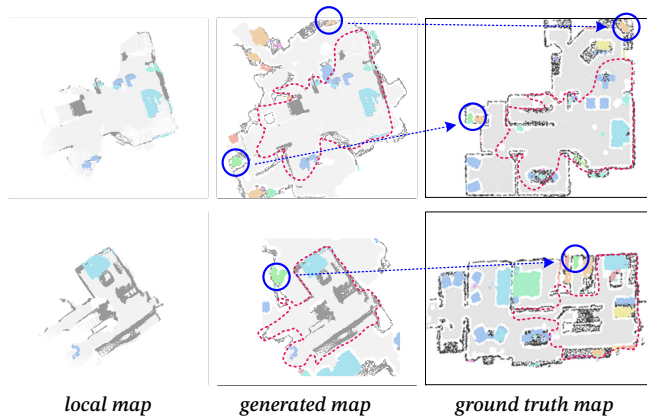


Figure 11: Generated maps during navigation.

Table II: The impact of prompting techniques on performance

Settings				Map Prediction	Navigation	
COT	Positive	Negative	Relation	Recall (%) \uparrow	SR (%) \uparrow	SPL (%) \uparrow
\times	\checkmark	\times	both	73.6	76.1	42.8
\times	\checkmark	\checkmark	both	74.4	77.9	43.7
\checkmark	\checkmark	\times	both	75.0	76.4	43.1
\checkmark	\checkmark	\checkmark	sem	75.1	76.7	43.5
\checkmark	\checkmark	\checkmark	spa	75.2	76.6	43.4
\checkmark	\checkmark	\checkmark	both	76.7	78.3	44.2

Table III: Ablation study.

Settings				Gibson		
GT	GTB	LLB	EXB	SR(%) \uparrow	SPL(%) \uparrow	DTS(m) \downarrow
\checkmark				91.7	72.3	0.38
	\checkmark			72.4	40.9	1.51
	\checkmark	\checkmark		75.1	42.4	1.45
	\checkmark	\checkmark	\checkmark	78.3	44.2	1.08

is effective, as it prevents being misled by low-confidence predictions from limited observations. The performance of the Local LLM bias largely depends on COT and positive-negative prompting techniques. The experiments we conducted in Table III demonstrate the effectiveness of extracting the association matrix M_{CS} from LLM by considering both spatial and semantic relations.

F. Comparisons with the related works.

We categorize existing ObjectNav works, evaluated on either the Gibson or MP3D datasets, into two approaches: 1) End-to-End: Directly outputs actions, primarily using reinforcement learning. 2) Modular-Based: Predicts a map-based long-term goal. These are listed in Table IV.

- DD-PPO: Utilizes end-to-end reinforcement learning with distributed training.
- Red-Rabbit: Enhances DD-PPO with auxiliary tasks for better sample efficiency and adaptability.
- THDA: Introduces "Treasure Hunt Data Augmentation" to improve rewards and adaptability in new scenes.
- Habitat-Web: Uses imitation learning with human demonstrations.
- FBE: Employs frontier-based exploration, creating a 2D occupancy map to find and approach targets.
- ANS: Implements modular reinforcement learning to improve coverage, similar to FBE for target identification.
- SemExp: A leading modular technique using reinforcement learning for effective long-term goal setting.
- STUBBORN: Uses a modular approach, assigning objectives to map corners and adapting through rotation, integrating target detections over frames.
- SGM uses a self-supervised MAE method based on the ViT architecture and integrates pretrained RoBERTa to

Table IV: Performance comparison with mainstream navigation methods.

Dataset	Metrics/Method	End-to-End					Modular-based						
		DD-PPO	Red-Rabbit	THDA	Habitat-web	RIM	FBE	ANS	SemExp	PONI	STUBBORN	SGM	DAR
Gibson	SR (%)↑	15.0	-	-	-	-	48.5	67.1	71.1	73.6	-	78.0	78.3
	SPL (%)↑	10.7	-	-	-	-	28.9	34.9	39.6	41.0	-	44.0	44.2
	DTS (m)↓	3.24	-	-	-	-	2.56	1.66	1.39	1.25	-	1.11	1.08
MP3D	SR (%)↑	8.0	34.6	28.4	35.4	50.3	29.5	21.2	28.3	27.8	31.2	37.7	42.6
	SPL (%)↑	1.8	7.9	11.0	10.2	17.0	10.6	9.2	10.9	12.1	13.5	14.7	15.3
	DTS (m)↓	6.94	-	5.62	-	-	5.00	6.31	6.06	5.63	5.01	4.93	5.02

merge LLM predictions, generating a semantic map of unknown areas. It selects the location with the highest target confidence in the map as the long-term goal.

In this study, although our DAR model employs a self-supervised approach, it achieves performance comparable to existing supervised methods across all metrics on various datasets. Notably, on the Gibson dataset, our DAR model surpasses the previous state-of-the-art self-supervised method by 3.5% in Success Rate (SR), 1.9% in Success weighted by Path Length (SPL), and reduces the Distance to Success (DTS) by 0.05 meters. It is important to note that a lower DTS value indicates better performance.

V. CONCLUSIONS

In this work, we propose a modular-based self-supervised method for the object goal navigation task, named DAR. We demonstrate the effectiveness of applying diffusion models to visual semantic reasoning. We first trained Denoising Diffusion Probabilistic Models based on the indoor semantic map dataset, and successfully generated high-quality and reasonable new map samples, indicating that the trained DDPM can learn the statistical distribution patterns of the spatial relationships between indoor objects, and we point out that this pattern is highly beneficial for improving the success rate and efficiency of the agent in the ObjectNav task. Subsequently, we use COT and positive-negative prompting techniques to query LLMs to obtain common sense knowledge, and incorporate it into the diffusion model’s reasoning process through the proposed *local bias* method. In summary, our DAR method explicitly leverages the structured knowledge from the knowledge graph extracted from LLM and implicitly utilizes the unstructured knowledge from the pre-trained diffusion model. A series of experiments have shown that the DAR method achieves comparable performance to previous methods.

REFERENCES

- [1] A. Chang, A. Dai, T. Funkhouser, M. Halber, M. Niessner, M. Savva, S. Song, A. Zeng, and Y. Zhang, “Matterport3d: Learning from rgb-d data in indoor environments,” *arXiv preprint arXiv:1709.06158*, 2017.
- [2] S. K. Ramakrishnan, A. Gokaslan, E. Wijmans, O. Maksymets, A. Clegg, J. Turner, E. Undersander, W. Galuba, A. Westbury, A. X. Chang *et al.*, “Habitat-matterport 3d dataset (hm3d): 1000 large-scale 3d environments for embodied ai,” *arXiv preprint arXiv:2109.08238*, 2021.
- [3] F. Xia, A. R. Zamir, Z. He, A. Sax, J. Malik, and S. Savarese, “Gibson env: Real-world perception for embodied agents,” in *Proceedings of the IEEE conference on computer vision and pattern recognition*, 2018, pp. 9068–9079.
- [4] M. Deitke, W. Han, A. Herrasti, A. Kembhavi, E. Kolve, R. Motaghi, J. Salvador, D. Schwenk, E. VanderBilt, M. Wallingford *et al.*, “Robothon: An open simulation-to-real embodied ai platform,” in *Proceedings of the IEEE/CVF conference on computer vision and pattern recognition*, 2020, pp. 3164–3174.
- [5] M. Savva, A. Kadian, O. Maksymets, Y. Zhao, E. Wijmans, B. Jain, J. Straub, J. Liu, V. Koltun, J. Malik *et al.*, “Habitat: A platform for embodied ai research,” in *Proceedings of the IEEE/CVF international conference on computer vision*, 2019, pp. 9339–9347.
- [6] X. Hu, Y. Lin, S. Wang, Z. Wu, and K. Lv, “Agent-centric relation graph for object visual navigation,” *IEEE Transactions on Circuits and Systems for Video Technology*, 2023.
- [7] H. Du, X. Yu, and L. Zheng, “Learning object relation graph and tentative policy for visual navigation,” in *Computer Vision—ECCV 2020: 16th European Conference, Glasgow, UK, August 23–28, 2020, Proceedings, Part VII 16*. Springer, 2020, pp. 19–34.
- [8] R. Druon, Y. Yoshizyasu, A. Kanazaki, and A. Watt, “Visual object search by learning spatial context,” *IEEE Robotics and Automation Letters*, vol. 5, no. 2, pp. 1279–1286, 2020.
- [9] B. Chen, J. Kang, P. Zhong, Y. Cui, S. Lu, Y. Liang, and J. Wang, “Think holistically, act down-to-earth: A semantic navigation strategy with continuous environmental representation and multi-step forward planning,” *IEEE Transactions on Circuits and Systems for Video Technology*, 2023.
- [10] B. Mayo, T. Hazan, and A. Tal, “Visual navigation with spatial attention,” in *Proceedings of the IEEE/CVF conference on computer vision and pattern recognition*, 2021, pp. 16 898–16 907.
- [11] D. S. Chaplot, D. P. Gandhi, A. Gupta, and R. R. Salakhutdinov, “Object goal navigation using goal-oriented semantic exploration,” *Advances in Neural Information Processing Systems*, vol. 33, pp. 4247–4258, 2020.
- [12] S. K. Ramakrishnan, D. S. Chaplot, Z. Al-Halah, J. Malik, and K. Grauman, “Poni: Potential functions for objectgoal navigation with interaction-free learning,” in *Proceedings of the IEEE/CVF Conference on Computer Vision and Pattern Recognition*, 2022, pp. 18 890–18 900.
- [13] S. Zhang, X. Yu, X. Song, X. Wang, and S. Jiang, “Imagine before go: Self-supervised generative map for object goal navigation,” in *Proceedings of the IEEE/CVF Conference on Computer Vision and Pattern Recognition*, 2024, pp. 16 414–16 425.
- [14] B. Yu, H. Kasaei, and M. Cao, “Frontier semantic exploration for visual target navigation,” in *2023 IEEE International Conference on Robotics and Automation (ICRA)*. IEEE, 2023, pp. 4099–4105.
- [15] M. Zhu, B. Zhao, and T. Kong, “Navigating to objects in unseen environments by distance prediction,” in *2022 IEEE/RSJ International Conference on Intelligent Robots and Systems (IROS)*. IEEE, 2022, pp. 10 571–10 578.
- [16] A. J. Zhai and S. Wang, “Peanut: Predicting and navigating to unseen targets,” in *Proceedings of the IEEE/CVF International Conference on Computer Vision*, 2023, pp. 10 926–10 935.
- [17] F. Zeng, W. Gan, Y. Wang, N. Liu, and P. S. Yu, “Large language models for robotics: A survey,” *arXiv preprint arXiv:2311.07226*, 2023.
- [18] B. Yu, H. Kasaei, and M. Cao, “L3mvn: Leveraging large language models for visual target navigation,” in *2023 IEEE/RSJ International Conference on Intelligent Robots and Systems (IROS)*. IEEE, 2023, pp. 3554–3560.
- [19] L. Sun, A. Kanazaki, G. Caron, and Y. Yoshizyasu, “Leveraging large language model-based room-object relationships knowledge for enhancing multimodal-input object goal navigation,” *arXiv preprint arXiv:2403.14163*, 2024.
- [20] J. Ho, A. Jain, and P. Abbeel, “Denoising diffusion probabilistic models,” *Advances in neural information processing systems*, vol. 33, pp. 6840–6851, 2020.
- [21] J. Achiam, S. Adler, S. Agarwal, L. Ahmad, I. Akkaya, F. L. Aleman, D. Almeida, J. Altenschmidt, S. Altman, S. Anadkat *et al.*, “Gpt-4 technical report,” *arXiv preprint arXiv:2303.08774*, 2023.
- [22] D. Shah, M. R. Equi, B. Osiński, F. Xia, B. Ichter, and S. Levine, “Navigation with large language models: Semantic guesswork as a heuristic for planning,” in *Conference on Robot Learning*. PMLR, 2023, pp. 2683–2699.
- [23] K. Yadav, R. Ramrakhya, S. K. Ramakrishnan, T. Gervet, J. Turner, A. Gokaslan, N. Maestre, A. X. Chang, D. Batra, M. Savva *et al.*,

- “Habitat-matterport 3d semantics dataset,” in *Proceedings of the IEEE/CVF Conference on Computer Vision and Pattern Recognition*, 2023, pp. 4927–4936.
- [24] J. Sun, J. Wu, Z. Ji, and Y.-K. Lai, “A survey of object goal navigation,” *IEEE Transactions on Automation Science and Engineering*, 2024.
- [25] S. Zhang, W. Li, X. Song, Y. Bai, and S. Jiang, “Generative meta-adversarial network for unseen object navigation,” in *European Conference on Computer Vision*. Springer, 2022, pp. 301–320.
- [26] R. Ramrakhya, D. Batra, E. Wijmans, and A. Das, “Pirlnav: Pretraining with imitation and rl finetuning for objectnav,” in *Proceedings of the IEEE/CVF Conference on Computer Vision and Pattern Recognition*, 2023, pp. 17 896–17 906.
- [27] X. Ye and Y. Yang, “Hierarchical and partially observable goal-driven policy learning with goals relational graph,” in *Proceedings of the IEEE/CVF Conference on Computer Vision and Pattern Recognition*, 2021, pp. 14 101–14 110.
- [28] H. Du, X. Yu, and L. Zheng, “Vtnet: Visual transformer network for object goal navigation,” *arXiv preprint arXiv:2105.09447*, 2021.
- [29] J. Ye, D. Batra, A. Das, and E. Wijmans, “Auxiliary tasks and exploration enable objectgoal navigation,” in *Proceedings of the IEEE/CVF international conference on computer vision*, 2021, pp. 16 117–16 126.
- [30] O. Maksymets, V. Cartillier, A. Gokaslan, E. Wijmans, W. Galuba, S. Lee, and D. Batra, “Thda: Treasure hunt data augmentation for semantic navigation,” in *Proceedings of the IEEE/CVF International Conference on Computer Vision*, 2021, pp. 15 374–15 383.
- [31] T. Gervet, S. Chintala, D. Batra, J. Malik, and D. S. Chaplot, “Navigating to objects in the real world,” *Science Robotics*, vol. 8, no. 79, p. eadf6991, 2023.
- [32] J. A. Sethian, “A fast marching level set method for monotonically advancing fronts,” *proceedings of the National Academy of Sciences*, vol. 93, no. 4, pp. 1591–1595, 1996.
- [33] Q. Zhao, L. Zhang, B. He, H. Qiao, and Z. Liu, “Zero-shot object goal visual navigation,” in *2023 IEEE International Conference on Robotics and Automation (ICRA)*. IEEE, 2023, pp. 2025–2031.
- [34] J. Chen, G. Li, S. Kumar, B. Ghanem, and F. Yu, “How to not train your dragon: Training-free embodied object goal navigation with semantic frontiers,” *arXiv preprint arXiv:2305.16925*, 2023.
- [35] S. Y. Gadre, M. Wortsman, G. Ilharco, L. Schmidt, and S. Song, “Cows on pasture: Baselines and benchmarks for language-driven zero-shot object navigation,” in *Proceedings of the IEEE/CVF Conference on Computer Vision and Pattern Recognition*, 2023, pp. 23 171–23 181.
- [36] G. Georgakis, B. Bucher, K. Schmeckpeper, S. Singh, and K. Daniilidis, “Learning to map for active semantic goal navigation,” *arXiv preprint arXiv:2106.15648*, 2021.
- [37] P. Dhariwal and A. Nichol, “Diffusion models beat gans on image synthesis,” *Advances in neural information processing systems*, vol. 34, pp. 8780–8794, 2021.
- [38] M. Zhao, F. Bao, C. Li, and J. Zhu, “Egsde: Unpaired image-to-image translation via energy-guided stochastic differential equations,” *Advances in Neural Information Processing Systems*, vol. 35, pp. 3609–3623, 2022.
- [39] A. Lugmayr, M. Danelljan, A. Romero, F. Yu, R. Timofte, and L. Van Gool, “Repaint: Inpainting using denoising diffusion probabilistic models,” in *Proceedings of the IEEE/CVF conference on computer vision and pattern recognition*, 2022, pp. 11 461–11 471.
- [40] O. Avrahami, O. Fried, and D. Lischinski, “Blended latent diffusion,” *ACM transactions on graphics (TOG)*, vol. 42, no. 4, pp. 1–11, 2023.
- [41] A. Q. Nichol and P. Dhariwal, “Improved denoising diffusion probabilistic models,” in *International conference on machine learning*. PMLR, 2021, pp. 8162–8171.
- [42] Y. Song and S. Ermon, “Generative modeling by estimating gradients of the data distribution,” *Advances in neural information processing systems*, vol. 32, 2019.
- [43] J. Wei, X. Wang, D. Schuurmans, M. Bosma, F. Xia, E. Chi, Q. V. Le, D. Zhou *et al.*, “Chain-of-thought prompting elicits reasoning in large language models,” *Advances in neural information processing systems*, vol. 35, pp. 24 824–24 837, 2022.
- [44] S. Chen, T. Chabal, I. Laptev, and C. Schmid, “Object goal navigation with recursive implicit maps,” in *2023 IEEE/RSJ International Conference on Intelligent Robots and Systems (IROS)*. IEEE, 2023, pp. 7089–7096.
- [45] O. Ronneberger, P. Fischer, and T. Brox, “U-net: Convolutional networks for biomedical image segmentation,” in *Medical image computing and computer-assisted intervention—MICCAI 2015: 18th international conference, Munich, Germany, October 5–9, 2015, proceedings, part III 18*. Springer, 2015, pp. 234–241.
- [46] K. He, X. Chen, S. Xie, Y. Li, P. Dollár, and R. Girshick, “Masked autoencoders are scalable vision learners,” in *Proceedings of the IEEE/CVF conference on computer vision and pattern recognition*, 2022, pp. 16 000–16 009.